Theory of light-induced drift. II. Circular-cylindrical geometry

Frank O. Goodman*
Department of Applied Mathematics, University of Waterloo, Waterloo, Ontario, Canada N2L 3G1
(Received 28 December 2001; published 17 June 2002)

Light-induced drift (LID) of a rarefied gas in a cell with circular-cylindrical geometry is studied, and exact solutions to the model rate equations are obtained, with exact analytical solutions for the case of surface LID (SLID); the special case of the limit of low radiation absorption by the gas in SLID is given particular attention. Many results are different from those of previous work. Emphasis is placed on considerations of comparison with experiment. This is part II of a series of papers, part I having studied LID with flat-plate geometry [F. O. Goodman, preceding paper, Phys. Rev. A **65**, 063409 (2002)].

DOI: 10.1103/PhysRevA.65.063410 PACS number(s): 34.50.Rk

I. INTRODUCTION

In part I (Ref. [1]) of this series of papers, the phenomenon of light-induced drift (LID) was discussed in detail, and an exact treatment of a model of surface LID (SLID) was presented for the case of flat-plate (FP) geometry in the limit of large cell length and cell width and in the free-molecule limit [1]. Motivated by previous work, both theoretical and experimental, certain specializations were made, particularly to cases of low radiation intensity absorption [1]. Emphasis was placed on relating theoretical results to experimental measurements, and considerations of applications to existing experimental data on FP SLID were presented [1].

In the present paper (''in the present paper'' is abbreviated from now on to ''here''), we consider a model of LID with circular-cylindrical (CC) geometry, specializing eventually to the case of CC SLID in the limit of large cell length, and in the free-molecule limit, for which an exact treatment is given. Specializations analogous to those in part I are also made here, emphasis again being placed on relating theory to experiment, and considerations of applications to existing CC SLID experimental data are presented.

In order to understand the material here, it is necessary for readers to have read and understood part I, and to have it at hand, as detailed references to its contents are made throughout. The following examples explain the notation used for brevity when references are made to part I: Eq. (4.10) of part I is denoted by (I. 4.10), Appendix H of part I is denoted by Appendix I-H, and so on; naturally, absence of the roman numeral I implies reference to an entity here.

Unless otherwise indicated, a symbol used in part I has the same meaning here. Important differences stem from the different geometry. The characteristic dimensional length [2] l_c^* was the cell thickness Z^* in part I, whereas it is the cell radius R^* here. The cell length X^* and cell width Y^* in part I are replaced by only the cell length X^* here; hence the dimensionless triplet $(X,Y,Z)=(X^*/Z^*,Y^*/Z^*,1)$ in part I is replaced here by the doublet $(X,R)=(X^*/R^*,1)$, leading to the obvious difference between the two meanings of X (neither Y nor Z appears in the CC analysis). Both the molecular system transition probability Ψ and the system parameter κ are different in FP and CC geometries: (I.H4) is replaced here by [3]

$$\Psi = 8/3X + O(\ln X/X^2), \tag{1.1}$$

and then Eq. (I.H3) implies that Eq. (I.H5) is replaced here by

$$\kappa \to 3\pi^{1/2}/4, \tag{1.2}$$

now nicely independent of X, and giving our standard (only) value of κ here. Also, the parameters a,g, and y have different definitions here from those in part I: Eqs. (I.E2), (I.E3), and (I.E2) are replaced, respectively, by

$$a=(\pi/2)Dq_0/C=(\pi/2)(\alpha_g+\alpha_e)q_0/\alpha_g\alpha_e, \tag{1.3}$$

$$g=(\pi/2)F\gamma/C=(\pi/2)\gamma/\alpha_e, \tag{1.4}$$

$$y=1-z. \tag{1.5}$$

The analog of the material in Secs. II–IV in Paper I is given here in Sec. II, and that of the material in Sec. V of Paper I appears in Sec. III. As in part I, care is taken to relate results to future possible experimental measurements. The analog of Sec VI of Paper I is Sec. IV, that is, considerations of applications to existing experiments, namely, the data in Refs. [4,5]. Section V is a brief conclusion.

II. THE MODEL: THE RATE EQUATIONS AND THEIR NUMERICAL SOLUTION, RELATIONSHIP WITH EXPERIMENTAL MEASUREMENTS

With the CC geometry used here, we consider initial free-molecule flow in an open circular-cylindrical tube, oriented with its axis in the x direction, which is also the direction in which the laser beam runs. The cylinder length/radius ratio, that is, its dimensionless length X, would be made large to enhance the SLID effect, and the limit of large X is understood here, leading to the absence of end effects. Characteristic dimensional quantities are chosen to give our dimensionless quantities, our choice giving

$$\hbar\omega = R = b = 2T/\mu = 1. \tag{2.1}$$

*Also at Department of Physics, University of Waterloo and the Guelph-Waterloo Physics Institute.

Unless otherwise made clear, the analysis is presented in terms of the resulting dimensionless quantities.

To build the CC Maxwell-Boltzmann rate equations (MBREs), we need the average frequency of collisions of molecules of velocity $\mathbf{v}$ with the surface, that is, $2V/\pi$, where $\mathbf{v}$ is written as

$$\mathbf{v}=(v_x,v_y,v_z)=(v_x,\mathbf{V}). \tag{2.2}$$

In order to enable the results here to be obtained directly from those in part I, we introduce replacements as follows:

$$M\rightarrow W, \tag{2.3}$$

$$|v_z|\rightarrow 2V/\pi, \tag{2.4a}$$

$$\beta_z\rightarrow B_V. \tag{2.4b}$$

In Eq. (2.3), the distribution $W(\mathbf{v})$ is the appropriate analog of the distribution $M(\mathbf{v})$ [1]:

$$W(\mathbf{v})=Vm(\mathbf{v})/\langle V\rangle_m=(2/\pi^2)Ve^{-v^2}; \tag{2.5}$$

in Eq. (2.4b), the quantities B_{Vj} are defined from the analog of Eq. (I.2.9a):

$$\langle V\rangle_m B_{Vj}=\langle V\rangle_j. \tag{2.6}$$

For example, the CC MBREs, that is, the analog of Eqs. (I.2.7), are just Eq. (I.2.7) with the replacements (2.3) and (2.4a), and the analog of Eq. (I.2.10) is just Eq. (I.2.10) with the replacements (2.4). The analog of Eq. (I.2.11a) is

$$B_{Vj}(t)=(2/\pi^{1/2})I_{Vj}(t)/I_{1j}(t), \tag{2.7}$$

where the integrals $I_{Vk}(t)$ are defined by the analog of Eq. (I.A1.2e):

$$I_{Vk}(t)=\int\int\int d^3\mathbf{v}Vf_k(\mathbf{v},t). \tag{2.8}$$

Section III of Paper I is essentially unchanged, the only important difference being the replacement of Z by R in Eq. (I.3.7). A trivial change occurs just before Eq. (I.3.3), that is, the absorbed radiation intensity is given here by $\pi^{-1}(dN_e/dt)_{\text{laser}}$ because the cross-sectional area of the cell is equal to Y in part I and π here; this affects nothing else because $N=\pi\rho X$ here instead of $N=\rho XY$ in Eq. (I.3.2). As we saw in Sec. I above, the parameter κ is more nicely defined [Eq. (1.2)] for CC geometry.

Section IV A of Paper I is also essentially unchanged, provided that the replacements (2.4) are made everywhere therein. Section IV B of Paper I needs modification because of the different geometry. In part I, it was natural to choose rectangular Cartesian coordinates (v_x,v_y,v_z) for the velocity space, and hence get Eqs. (I.4.7) and (I.4.8), for example. Here, it is natural to choose cylindrical polar coordinates (v_x,V,ζ), defined from Eq. (2.2) and

$$\mathbf{V}=V(\cos\zeta,\sin\zeta), \tag{2.9}$$

and to replace Eq. (I.4.7) by

$$\mathbf{s}=(s_1,s_2,s_3)=(\text{erf}v_x,e^{-V^2},\zeta/2\pi), \tag{2.10}$$

which leads to replacing Eq. (I.4.8) by

$$m(\mathbf{s})=\tfrac{1}{2}:-1<s_1<1,\quad 0<s_{2,3}<1. \tag{2.11}$$

With pure SLID, the quantity which integrated out trivially in part I was v_y, that is, s_y, whereas here it is ζ, that is, s_3.

III. EXACT ANALYTICAL STEADY-STATE SOLUTION FOR SLID

A. The general case

For Sec. V of Paper I, in which the subscript z was dropped from β, the replacement (2.4a) remains as is but Eq. (2.4b) becomes simply $\beta\rightarrow B$, and the integral I_{Vj} is now important instead of the integral I_{zj}, Eq. (I.5.3c) having the analog

$$c_eB_e=(2/\pi^{1/2})I_{Ve}. \tag{3.1}$$

The closed-form results for the eight integrals I_{1j}, I_{qj}, I_{xj}, and I_{Vj} are given in Appendix A, and it is important to recall definitions made in part I, for example, those of G_ξ,H_ξ, and w in Eqs. (I.E5) and (I.E6), and of $d(\text{erf})$ and $d(\text{exp})$ in Eqs. (I.4.10) and (I.E4); the new definitions (1.3)–(1.5) of a,g, and y must also be recalled, and that Eq. (A2) of W_j noted. The exact results for I_{1e}, I_{qd}, and I_{xs} are given in Appendix B.

B. The special case $a\rightarrow 0$ in the general case

With CC geometry, there are no problems with the two limits $a\rightarrow 0$, $g\rightarrow 0$, as there are with FP geometry, because they now commute, and the only special case which needs reporting is that in this section. The analogs of Eq. (I.5.5) are as follows:

$$\frac{I_{1e}}{a}\rightarrow\frac{[2y+\pi^{1/2}(\pi^{1/2}z-2gy)H_g]}{[2gy+\pi^{1/2}(z-2g^2yH_g)]}\frac{\alpha_g}{\Sigma\alpha}\frac{d(\text{erf})}{2}, \tag{3.2a}$$

$$\frac{I_{xs}}{a}\rightarrow H_g\frac{\Delta\alpha}{\Sigma\alpha}\frac{d(\text{exp})}{2}, \tag{3.2b}$$

$$\frac{I_{qd}}{a}\rightarrow\frac{\alpha_g\alpha_e}{\Sigma\alpha}\frac{d(\text{erf})}{\pi}, \tag{3.2c}$$

and those of Eqs. (I.5.6) and (I.5.8) are

$$\delta\rightarrow\frac{3\pi^{3/2}H_g}{8}\frac{d(\text{exp})}{d(\text{erf})}\frac{\Delta\alpha}{\alpha_g\alpha_e}\rightarrow\frac{3\pi^2v_LH_g}{8}\frac{\Delta\alpha}{\alpha_g\alpha_e}. \tag{3.3}$$

Results for $g=0$ are trivially obtained ($H_g=1$) from Eqs. (3.2) and (3.3), and the analog of Eq. (I.5.11) is [2]

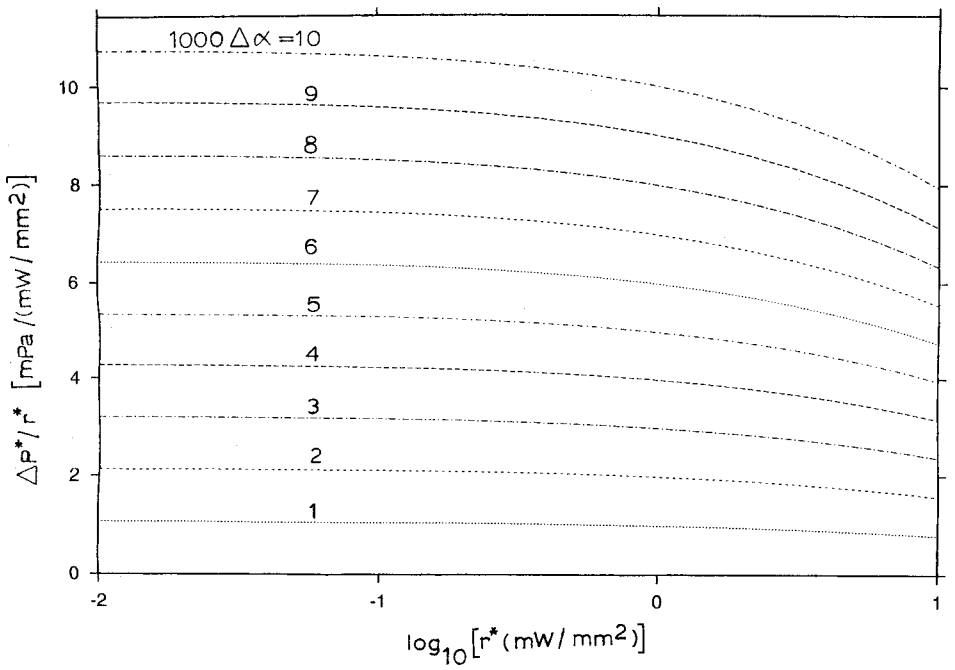

FIG. 1. Dependence on r of $\Delta P/r$ for the ten values of $\Delta\alpha$ given by $1000\Delta\alpha=1(1)10$. The parameters are $\alpha_g=1$, $z=0.5$, $\gamma=0$, $v_a=0$, $v_b=\infty$, with a varying as necessary to produce the results. The meanings of the symbols are as follows: r is the absorbed laser radiation power intensity, ΔP is the across-cell pressure difference, $\Delta\alpha=\alpha_g-\alpha_e$, where $\alpha_{g,e}$ are the ground- and excited-state accommodation coefficients, z is the diffuse-scattering quenching fraction, γ is the spontaneous decay-rate parameter, $[v_a,v_b]$ is the interval of v_x in which the laser excitation function $q(v_x)$ equals q_o, and a is defined by Eq. (1.3).

$$\frac{(\Delta P^*/\mathrm{mPa})}{(r^*\mathrm{mm}^2/\mathrm{mW})}\approx 1068\frac{d(\exp)}{d(\mathrm{erf})}\frac{\Delta\alpha}{\alpha_g\alpha_e}\left(\frac{\mu^*}{30\ \mathrm{amu}}\right)^{1/2}\times\left(\frac{T^*}{300\ \mathrm{K}}\right)^{1/2}\left(\frac{\lambda^*}{10\ \mu\mathrm{m}}\right), \tag{3.4a}$$

$$\frac{1000c_e/(r^*\mathrm{mm}^2/\mathrm{mW})}{(1+2y/\pi z)}\approx\frac{14.24}{\alpha_e}\left(\frac{\mathrm{Pa}}{P^*}\right)\left(\frac{R^*/\mathrm{mm}}{X^*/10\ \mathrm{cm}}\right)\times\left(\frac{\mu^*}{30\ \mathrm{amu}}\right)^{1/2}\left(\frac{T^*}{300\ \mathrm{K}}\right)^{1/2}\left(\frac{\lambda^*}{10\ \mu\mathrm{m}}\right), \tag{3.4b}$$

$$100a\approx\left(\frac{1.606\Sigma\alpha}{\alpha_g\alpha_e d(\mathrm{erf})}\right)\left(\frac{r^*\mathrm{mm}^2}{\mathrm{mW}}\right)\left(\frac{R^*/\mathrm{mm}}{X^*/10\ \mathrm{cm}}\right)\left(\frac{\mathrm{Pa}}{P^*}\right)\times\left(\frac{\mu^*}{30\ \mathrm{amu}}\right)^{1/2}\left(\frac{T^*}{300\ \mathrm{K}}\right)^{1/2}\left(\frac{\lambda^*}{10\ \mu\mathrm{m}}\right). \tag{3.4c}$$

With our standard quantities (excluding ΔP^* and r^*), we show exact results for $\Delta P/r$ as a function of r for ten values of $\Delta\alpha$ in Fig. 1, using the parameters listed in the caption. Figure 2 shows analogous exact results for the seven values of γ used in Fig. 3 of Ref. [1], again using the parameters listed in the caption.

IV. APPLICATIONS TO EXPERIMENTS

Section VI of Paper I is unchanged down to Eq. (I.6.2), with the reported values of $C_e/(r/\rho)$ for CC geometry coming from Refs. [4,5], with their ν_k and ν assumed negligible:

$$C_e/(r/\rho)=\pi^{1/2}/X, \tag{4.1}$$

which is the analog of Eq. (I.6.3); that of Eq. (I.6.4) is

$$\Delta=X\delta/\pi^{1/2}, \tag{4.2}$$

with the low-intensity special case of δ given by Eq. (3.3).

The analog of Eq. (I.6.5) is

$$\tilde{\Delta}=\tfrac{3}{4}\pi^{1/2}\phi(\Omega)X\widetilde{\Delta\alpha}, \tag{4.3}$$

and that of Eq. (I.6.7) is

$$\frac{1000\Delta\alpha}{\Delta}\rightarrow\frac{8000}{3\pi X}\frac{d(\mathrm{erf})}{d(\exp)} \tag{4.4a}$$

$$\rightarrow\frac{8000}{3\pi^{3/2}Xv_L} \tag{4.4b}$$

with the value (1.2) of κ, leading to the following analog of Eq. (I.6.8):

$$\frac{\Delta\alpha}{\widetilde{\Delta\alpha}}\rightarrow\frac{2}{\pi}\frac{\phi(\Omega)}{v_L}. \tag{4.5}$$

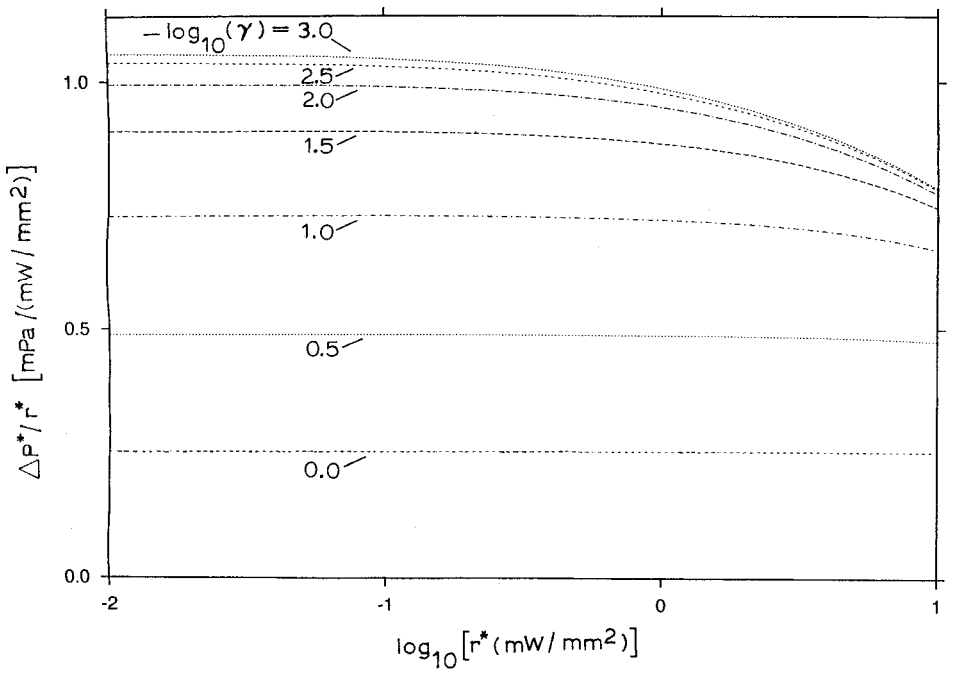

FIG. 2. Dependence on r of $\Delta P/r$ for the seven values of γ given by $-\log_{10}\gamma = 0(0.5)3$. The parameters are as in Fig. 1 except that $\alpha_e = 0.999$, $z = 0$, and $\gamma > 0$. The meanings of the symbols are as in Fig. 1.

The simplification (I.6.9) holds here also [4,5]. The analog of Eq. (I.6.10) is

$$\frac{\Delta\alpha}{\widetilde{\Delta\alpha}} \to \frac{2}{\pi H_g}\frac{\phi(\Omega)}{v_L}, \tag{4.6}$$

of which Eq. (4.5) is the special case with $g = 0$.

We now use the CC data of Refs. [4,5] to infer values of $\Delta\alpha$ and compare them to those, $\widetilde{\Delta\alpha}$, obtained therein, again using Eq. (I.6.9) throughout the working.

Reference [4] contains results for CC geometry on the $R(4,3)$ transition of $^{13}CH_3F$ on teflon, quartz, and stainless steel surfaces, and on the $P(5)$ transition of OCS on a quartz surface [6]. Table I shows a comparison of results from Eq. (4.4) with those of Table I of Ref. [4]; we use parameters $v_L = 0.50$ and $X = 400$. It seems that their [4] results for $\widetilde{\Delta\alpha}$ in column 4 of their Table I are not consistent with their stated [4] parameters $\phi(\Omega) \approx 0.50$ and $X \approx 400$, and so column 5 of our Table I has been calculated by the present author, assuming that their parameters are as stated. [It is interesting that the different choice $\phi(\Omega) = \pi^{-1/2}$, which in fact corresponds to our $d(\exp)/d(\mathrm{erf}) = 1$ according to Eqs. (I.5.7) and (I.6.9), renders the entries in their [4] Table I consistent.] Columns 5 and 6 of our Table I are now consistent with Eq. (4.5), but this would not be so if the $\widetilde{\Delta\alpha}$ from Ref. [4] were used instead.

TABLE I. Comparison of results from Eq. (4.4) with those of Ref. [4] with CC geometry; column 5 has been calculated here as described in Sec. IV.

Molecule	Transition	Surface	$-\tilde{\Delta}$	$-1000\widetilde{\Delta\alpha}$	$-1000\Delta\alpha$
$^{13}CH_3F$	$R(4,3)$	Teflon	0.74	2.8	1.8
$^{13}CH_3F$	$R(4,3)$	Quartz	0.57	2.1	1.4
$^{13}CH_3F$	$R(4,3)$	Steel	0.30	1.1	0.72
OCS	$P(5)$	Quartz	−0.16	−0.60	−0.38

Reference [5] contains results for CC geometry on $P(k+1)$ and $R(k)$ transitions, with $k = 0(1)3$, of HF on LiF and stearic acid surfaces [6]. The experimental values of $\tilde{\Delta}$ are not quoted (although they may be inferred from their [5] Figs. 4 and 5), but their [5] calculated values of $\widetilde{\Delta\alpha}$ are given in their Fig. 6. However, if all is well, reexamining their data should not be necessary here, as our values of $\Delta\alpha$ are presumably just their values [6] multiplied by $2/\pi$ according to Eq. (4.5), although the problem with the results from Ref. [4] in column 5 of Table I, discussed in the previous paragraph, should perhaps be borne in mind.

If their [5] procedure of inferring the vibrational and rotational parts of $\Delta\alpha$ (we drop the tilde now) separately via their assumption (4) were followed here, then presumably our results would be those in their Table I [6], also multiplied by $2/\pi$. Their results [5] suggest the following attempt at correlating their data:

$$\alpha(v,J) \approx \alpha(0,0) + v\,\alpha_v(0,0) + J\alpha_J(0,0), \tag{4.7}$$

that is, the start (the first three terms) of a Taylor series about the origin, with partial derivatives α_v and α_J, ignoring the discrete nature of v and J. Our Eq. (4.7) is nothing more than a special case of their [5] assumption (4), but it has more physical content if it were to fit the data well, as is suggested by their Fig. 7. In fact, the overall fit is good, and we infer, by means of nonsophisticated averaging over the data in their [5] Table I, that $1000\alpha_v(0,0) \approx -0.7$ for both surfaces, and

that $1000\alpha_J(0,0)\approx 1.3$ and 1.9, respectively, for the LiF and stearic acid surfaces. If their [5] "cross terms" are interpreted as the second-order term $2vJ\alpha_{vJ}(0,0)$ of the Taylor series started in Eq. (4.7), then (because the first partial derivatives are so small) it is perhaps not surprising that they, as well as any other higher-order terms, are unnecessary in Eq. (4.7) or their [5] assumption (4). It is a pity that more information about the $\alpha(0,0)$ values, other than that they are expected [5] to be close to 1, is not available.

V. CONCLUSION

The first paragraph of Sec. VII in Paper I applies here also. With hindsight, it is clear that CC geometry is far more preferable than FP geometry for LID experiments, because of their resulting much easier and cleaner interpretation. The complicated dependencies on X,Y, and a with FP geometry do not exist with CC geometry: for example, the direct proportionality of ΔP to absorbed radiation intensity (in the low-intensity limit) leads to an obvious advantage of CC geometry; these remarks concerning CC versus FP geometry are further illustrated by comparison of Figs. 1 and 2 with Figs. 2 and 3 of Paper I, respectively.

Experimenters using CC geometry should always bear in mind the large-X assumption made in the computations, but they [4,5] are clearly well aware of this point. An estimate of how large X needs to be for validity of at least part of our analysis may be gleaned from the fact [3] that the second term in the expression (1.1) for Ψ is equal to $-3\ln X/4X$ times the first term. For example, $X=24$ and 60 give errors of about 10% and 5%, respectively, while the experimental [4,5] value $X\approx 400$ gives an error of only about 1% , which is obviously adequate.

ACKNOWLEDGMENTS

The author is greatly indebted to Professor A. D. Streater and Professor M. A. Vaksman for discussions on LID, and to Professor C. B. Collins for discussions on the analytical properties of the function $G(u)$. The work was supported by the Natural Sciences and Engineering Research Council of Canada.

APPENDIX A: INTEGRALS IN THE ANALYTICAL SOLUTION FOR SLID WITH CC GEOMETRY

With the definitions (I.E8) and [7]

$$U_\xi = 1-\pi^{1/2}\xi H_\xi, \tag{A1}$$

$$W_j = aX_j + gY_j, \tag{A2}$$

where we note that Eq. (A2) is different from Eq. (I.E7), the results of calculating the required integrals may be written as follows:

$$I_{1j} = A_j/C + \pi^{1/2}W_jH_w d(\mathrm{erf}) + \pi^{1/2}gJY_jH_g, \tag{A3a}$$

$$I_{qj} = (A_j/2C + \pi^{1/2}W_jH_w)q_0 d(\mathrm{erf}), \tag{A3b}$$

$$I_{xj} = (W_jH_w - gY_jH_g)d(\exp), \tag{A3c}$$

$$I_{Vj} = \pi^{1/2}A_j/2C + W_jU_w d(\mathrm{erf}) + gJY_jU_g. \tag{A3d}$$

APPENDIX B: EXACT RESULTS FOR THE GENERAL CASE OF SLID WITH CC GEOMETRY

In the notation (I.F1), with the definitions (I.E8) and

$$\Delta H = H_g - H_w, \tag{B1}$$

$$K = 2g^2yH_g - z, \tag{B2}$$

the results may be written as follows:

$$I_{1e}^{(\mathrm{num})} = (2y - \pi^{1/2}\{y[2aH_w + 2gH_g - g\Delta H d(\mathrm{erf})] - \pi^{1/2}[z + agyJH_g]H_w\})a\alpha_g d(\mathrm{erf}), \tag{B3}$$

$$I_{qd}^{(\mathrm{num})} = 2\{2gy - \pi^{1/2}[K + 2agyH_w - g^2y\Delta H d(\mathrm{erf}) + \pi^{1/2}a(z - g^2yJH_g)H_w]\}a\alpha_g\alpha_e d(\mathrm{erf}), \tag{B4}$$

$$I_{xs}^{(\mathrm{num})} = \{gy[2H_w + \Delta H d(\mathrm{erf})] - \pi^{1/2}[K + agyH_g d(\mathrm{erf})]H_w\}a\Delta\alpha d(\exp), \tag{B5}$$

$$I_{1e}^{(\mathrm{den})} = 4y[g\Sigma\alpha + a\alpha_g d(\mathrm{erf})] - \pi^{1/2}\{2K\Sigma\alpha + [2y(2agH_w\Sigma\alpha + 2a^2H_w\alpha_g + agH_g\Delta\alpha - g^2\Delta H\Sigma\alpha) - agy\Delta H\Delta\alpha d(\mathrm{erf})]d(\mathrm{erf}) - \pi^{1/2}(z + agyJH_g)H_w a\Delta\alpha d(\mathrm{erf})\}, \tag{B6}$$

$$I_{xs}^{(\mathrm{den})} = I_{qd}^{(\mathrm{den})}/\pi = I_{1e}^{(\mathrm{den})}. \tag{B7}$$

[1] F.O. Goodman, preceding paper, Phys. Rev. A **65**, 063409 (2002).
[2] Remember that dimensional quantities are asterisked (Ref. [1]).
[3] A.S. Berman, J. Appl. Phys. **36**, 3356 (1965).
[4] G.J. van der Meer, B. Broers, R.W.M. Hoogeveen, and L.J.F. Hermans, Physica A **182**, 47 (1992).
[5] E.J. van Duijn, R. Nokhai, L.J.F. Hermans, A.Yu. Pankov, and S.Yu. Krylov, J. Chem. Phys. **107**, 3999 (1997).
[6] Remember that the other workers use the definition $\Delta\alpha = \alpha_e - \alpha_g$, that is, the negative of that used here.
[7] Remember that ξ is a dummy variable (Ref. [1]).